AD-A274 794

# REPORT DOCUMENTATION PAGE

Form Approved
OMB No 0704-0188



| 1 AGENCY USE ONLY (Leave blank) | 2 REPORT DATE | 3 REPORT TYPE AND DATES COVERED |
|---|---|---|
| | December 1993 | Professional Paper |

4 TITLE AND SUBTITLE

SIMULATED ROTATIONAL RAMAN CONVERSION IN H2, D2, AND HD

5 FUNDING NUMBERS

PR: ZF07
PE: 0602936N
WN: DN300196

6 AUTHOR(S)

F. Hanson and P. Poirer

7 PERFORMING ORGANIZATION NAME(S) AND ADDRESS(ES)

Naval Command, Control and Ocean Surveillance Center (NCCOSC)
RDT&E Division
San Diego, CA 92152-5001

8 PERFORMING ORGANIZATION REPORT NUMBER

9 SPONSORING/MONITORING AGENCY NAME(S) AND ADDRESS(ES)

Office of Chief of Naval Research
OCNR-20T
Arlington, VA 22217

10 SPONSORING/MONITORING AGENCY REPORT NUMBER



11 SUPPLEMENTARY NOTES

12a DISTRIBUTION/AVAILABILITY STATEMENT

Approved for public release; distribution is unlimited.



13. ABSTRACT (Maximum 200 words)

This paper describes single-pass rotational Raman conversion efficiencies at 532 nm measured in $H_2$, $D_2$, and HD with different focusing geometries and over a range of pressures. Maximum efficiencies of 80%, 75%, and 64% were obtained at the first Stokes transition in these gases.

Published in *IEEE J. Quantum Electronics*, August 1993, pp. 2342-2345.



14. SUBJECT TERMS

optics
non-linear optics
lasers

15. NUMBER OF PAGES

16. PRICE CODE

| 17 SECURITY CLASSIFICATION OF REPORT | 18. SECURITY CLASSIFICATION OF THIS PAGE | 19 SECURITY CLASSIFICATION OF ABSTRACT | 20. LIMITATION OF ABSTRACT |
|---|---|---|---|
| UNCLASSIFIED | UNCLASSIFIED | UNCLASSIFIED | SAME AS REPORT |

| 21a NAME OF RESPONSIBLE INDIVIDUAL | 21b TELEPHONE (Include Area Code) | 21c OFFICE SYMBOL |
|---|---|---|
| F. Hanson | (619) 553-5720 | Code 843 |

# Stimulated Rotational Raman Conversion in $H_2$, $D_2$, and HD

Frank Hanson and Pete Poirier

*Abstract*—**Single-pass rotational Raman conversion efficiencies at 532 nm have been measured in $H_2$, $D_2$, and HD with different focusing geometries and over a range of pressures. Maximum efficiencies of 80%, 75%, and 64% were obtained at the first Stokes transition in these gases.**

## I. Introduction

THERE is considerable interest in finding efficient and long-lived laser sources for many applications in the marine environment such as communication and remote sensing. Narrow-band atomic resonance filters [1] or tunable filters that operate at strong Fraunhofer lines [2] have been proposed as methods to reduce the strong solar background at the receivers in such systems. However, a major problem with this technology has been to find a suitable laser source with the appropriate wavelength to match up with the best filter/receivers in the blue-green spectral region where the transmission in sea water is peaked. Laser diode pumped, neodymium based solid-state lasers have been widely demonstrated in the last few years to exhibit efficiencies and lifetimes that are substantially improved over comparable flashlamp pumped lasers. It seems clear that diode pumped laser systems will become increasingly important in many military and commercial applications. Unfortunately, there are no practical diode pumped solid-state lasers that operate directly in the blue-green spectral region. In order to exactly match one of the preferred wavelengths, some combination of nonlinear frequency conversion and/or tunable laser pumping is therefore required. Stimulated Raman scattering occurs in a wide variety of materials and can be a highly efficient means of frequency shifting laser sources.

We have recently examined possible laser systems based on the neodymium $^4F_{3/2} \rightarrow {}^4I_{9/2}$ transition with a combination of frequency doubling and Raman shifting that could potentially reach the strong $H_\beta$ Fraunhofer dip at 486 nm [3]. This line is $\sim 1$ Å wide and the solar irradiance at the minimum is only 15% of the continuum level. Such an approach would require relatively small Raman shifts such as the rotational Stokes shift in hydrogen. It is known that efficient stimulated rotational Raman scattering (SRRS) can occur in $H_2$ and $D_2$ [4], [5]; however, experimental details such as optimum gas pressure and pump thresholds are not available. In this work, we report a systematic characterization of SRRS in the three molecular hydrogen isotopes, $H_2$, $D_2$, and HD.

Manuscript received June 13, 1992; revised December 6, 1992.

The authors are with NCCOSC/RDT&E Division, Code 843, San Diego, CA 92152.

IEEE Log Number 9210249.

## II. Theory

For these simple diatomic molecules, the energy in $cm^{-1}$ of the rotational level $J$ in the ground vibration state is given to good accuracy by [6]

$$E_J = hc[B_o J(J+1) - D_o J^2(J+1)^2]. \quad (1)$$

Values of the rotational constants [7] for the three common molecular isotopes of hydrogen are given in Table I. In the homonuclear diatomics $H_2$ and $D_2$, two forms, ortho and para, are used to distinguish molecules depending on the total nuclear spin. The ortho form generally refers to the more abundant species, and for hydrogen, these are the molecules having a symmetric nuclear spin function and antisymmetric rotational functions. Thus ortho hydrogen can have only odd $J$ values and para hydrogen even $J$ values. For $D_2$, the opposite is true and the even $J$ states are more common. Transitions between these classes are usually quite slow and require some magnetic perturbation. There are no symmetry restrictions for HD; thus all $J$ states are equally accessible.

Raman transitions $J \rightarrow J+2$ give rise to different Stokes lines $S(J)$ in the scattered light spectrum on the long wavelength side of the pump. The rotational Raman gain at the Stokes wavelength is proportional to the incident pump intensity and is largest for Stokes light having circular polarization opposite to the pump light. We consider only the factors affecting the relative steady-state rotational Raman gain at the Stokes wavelength $\lambda_s$ for the different hydrogen molecules. These are given by [8]

$$g = \frac{\Delta N_J}{\lambda_s \Delta \nu} \frac{(J+1)(J+2)}{(2J+1)(2J+3)}. \quad (2)$$

Here, $\Delta N_J$ is the temperature dependent population factor between initial state $J$ and final state $J+2$,

$$\Delta N_J = N_J - N_{J+2} \frac{2J+1}{2J+3} \quad (3)$$

and

$$N_J = \frac{\rho}{Z_R}(2J+1)e^{-E_J/kT} \sum_{T_J} (2T_J + 1) \quad (4)$$

is the equilibrium population of the $J$ level for a total

TABLE I
SPECTROSCOPIC PARAMETERS FOR HYDROGEN ISOTOPES FROM [7]

| Hydrogen Molecule | $B_v$(cm$^{-1}$) | $D_v$ (cm$^{-1}$) | $T_J$ | Nuclear Degeneracy | $J$ Values Allowed |
|---|---|---|---|---|---|
| $H_2$ | 59.3392 | 0.04599 | 0 | 1 | even |
| | | | 1 | 3 | odd |
| $D_2$ | 29.9105 | 0.01134 | 0, 2 | 6 | even |
| | | | 1 | 3 | odd |
| HD | 44.6678 | 0.02592 | | | all |

TABLE II
DENSITY-BROADENING COEFFICIENTS $\mathcal{B}$ (MHz/amagat) AT 293 K FROM [11]

| Gas | $S(0)$ | $S(1)$ | $S(2)$ | $S(3)$ | $S(4)$ |
|---|---|---|---|---|---|
| $H_2$ | 83.9 | 104 | 74.1 | 75.9 | 46.4 |
| $D_2$ | 168 | 134 | 124 | 102 | 85.7 |
| HD | 857 | 759 | 660 | 544 | 402 |

number density $\rho$. The summation is over the allowed values of the total nuclear spin $T_J$, and

$$Z_R = \sum_{JT_J} (2T_J + 1)(2J + 1)e^{-E_J/kT} \quad (5)$$

is the rotational partition function.

The linewidth $\Delta\nu$ depends on temperature and density and is in general, different for each transition in each of the gases. At low density the Raman lineshape is Gaussian due to Doppler broadening. At densities above a critical value, the lineshape is Lorentzian and the linewidth (FWHM) for each transition can be described as the sum of a diffusion term and a density-broadening term [9], [10]

$$\Delta\nu = A/\rho + B\rho. \quad (6)$$

The critical density is less than 1 amagat ($2.69 \times 10^{19}$ cc$^{-1}$) for the first few Stokes lines in $H_2$ and is expected to be similar for the heavier isotopes. The model predicts a minimum linewidth due to collisional narrowing for $\rho = (A/B)^{1/2}$. This occurs for the $S(1)$ line of $H_2$ at 0.23 amagat. Above one amagat, the broadening of the first few lines is essentially linear in density due to the term involving $\mathcal{B}$. This coefficient has been measured [11] for the first few transitions in each of the gases and values are listed in Table II. B is much larger for HD than for either $H_2$ or $D_2$, due to the relatively strong dipole term in the intermolecular potential. The linear broadening generally decreases with increasing $J$ as the energy level spacing becomes larger.

The steady-state gain predicted from (2) using this model scales as $\rho/\Delta\nu = \rho^2/(A + B\rho^2)$, which increases with density and gradually reaches a limiting value proportional to $1/B$ at higher density. All of the experiments described below were done with gas densities greater than 1 amagat, the density at 760 torr, $T = 0°C$ for an ideal gas, and therefore the Raman linewidth should be approximately $B\rho$. To get an indication of the relative gain to be expected for the first few Raman lines, we have calculated the gain factor $g$ from the population statistics of the rotational levels and with the assumption that $\Delta\nu = B\rho$. The results at 300 K are shown in Fig. 1. The $S(1)$ line in $H_2$ at 587 cm$^{-1}$ is clearly expected to have the largest gain. In $D_2$ and HD, the largest gain is predicted for $S(2)$ at 414.5 cm$^{-1}$ and $S(1)$ at 443 cm$^{-1}$, respectively. The gain in HD is dramatically reduced due to the much larger line broadening. At lower temperatures, the dominate line will become $S(0)$ for each of the isotopes. This should happen at ~100 K for $H_2$ and ~200 K for $D_2$ and HD [3].

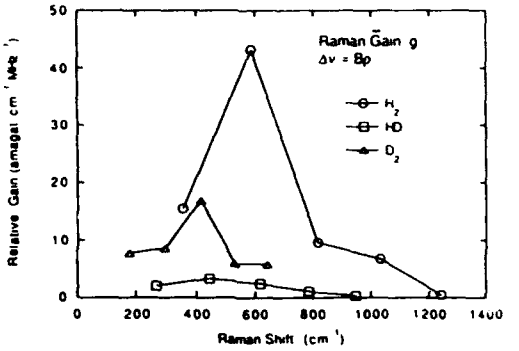


Fig. 1. Calculated relative steady-state rotational Raman gain spectrum at 300 K.

For temporal pump pulse widths on the order of or shorter than the rotational relaxation time $\tau = 1/\Delta\nu$, the stimulated Raman scattering is in the transient regime [12]. The Raman gain is less in the transient regime and asymptotically approaches the steady-state gain as the pump pulse width increases relative to $\tau$. Since the pump pulse width for these experiments is ~10 ns, we expect the effective gain in $H_2$ and $D_2$ to increase with density up to several amagats. The gain in HD is already close to the steady-state value at 1 amagat and should show less pressure dependence.

## III. EXPERIMENTAL

The Raman conversion efficiencies were measured in a single pass cell as shown in Fig. 2. The $H_2$ purity was 99.999%. Both $D_2$ and HD were obtained from Cryogenic Rare Gas Laboratories with purity of 99.95% and 97%, respectively. The pump source was a Q-switched, frequency doubled Nd:YAG laser (Quanta-Ray model DCR-3G) with a near diffraction limited beam. The laser could be operated with or without narrow line injection seeding, giving a spectral output of $< 0.001$ cm$^{-1}$ or $< 1$ cm$^{-1}$, respectively. The experiments were performed with the narrow line pump source although we found no significant difference in Raman conversion by using the seeder. This insensitivity to pump bandwidth is expected and has been observed before by Trutna, *et al.* [13]. For forward Raman scattering, the acceptance bandwidth is generally very large.

The nominally collimated pump beam was circularly polarized with a $\lambda/4$ plate and focused near the center of the 1-m long gas cell using either a 50-cm or 100-cm lens.

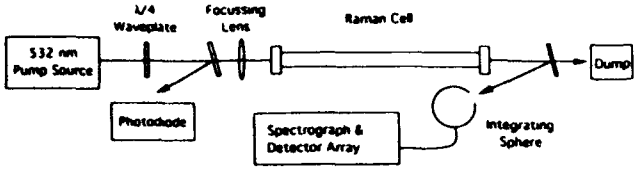


Fig. 2. Experimental setup to measure Raman conversion efficiency.

In these measurements, the intensity at 532 nm was varied by adjusting the lamp energy, which did cause small changes in effective focal length and pulse width. Since the laser was generally operated somewhat below maximum output, the pump was slightly diverging before the focusing lens. The beam width was ~6 mm at the lens. The pulse width (FWHM) varied from 12 ns at 10 mJ to 7 ns at 200 mJ. Beam splitting plates were used at near normal incidence before and after the Raman cell to sample the pump and output beams. A photodiode was calibrated to give the pump energy incident on the focusing lens. These are the values given in the figures below—they are not corrected for the transmission of the lens and cell window which was ~85%. All of the light exiting the cell was captured by an integrating sphere from which a fiber optic bundle brought a sample of the output to a 0.5-m spectrograph and silicon detector array. The Raman shifted output beam was found to be generally uniform over a solid angle somewhat larger than that of the diverging pump beam, although we did not attempt to quantify the angular distribution.

The Raman conversion efficiencies described below were the fraction of the pump light at 532 nm entering the cell that was converted to the first rotational Stokes wavelength $S_1$. Various losses due to surface reflections were ignored. The wavelength dependent response of the integrating sphere, fiber optic, and spectrograph was calibrated with a tungsten halogen lamp over a range around the pump wavelength from the first anti-Stokes ($AS_1$) to a few Stokes orders ($S_n$). At low pump energy, all of the output was contained in this region and the spectrograph could be calibrated with respect to the input pump energy. With increasing pump energy, and especially with the longer focal length lens, many lines might be observed in the output. Vibrational scattering could generally be observed at sufficiently high input. The conversion efficiency at $S_1$ was taken as the ratio of the average energies over several shots (not the average of the ratios from each shot). This causes a slight underestimation of energy threshold since there were relatively large fluctuations of pump energy at the low end.

The best Raman conversion was obtained with $H_2$ as expected from the population statistics and since the gain line is the narrowest. The efficiencies of the $S_1(1)$ transition at 549 nm are shown in Fig. 3. With a 50 cm focusing lens, conversion of 75% to 80% was obtained throughout the pressure range studied, 800 torr to 4500 torr. The maximum conversion was slightly better at the lower pressure. As the pressure was increased, the threshold decreased and the width of the conversion curve became

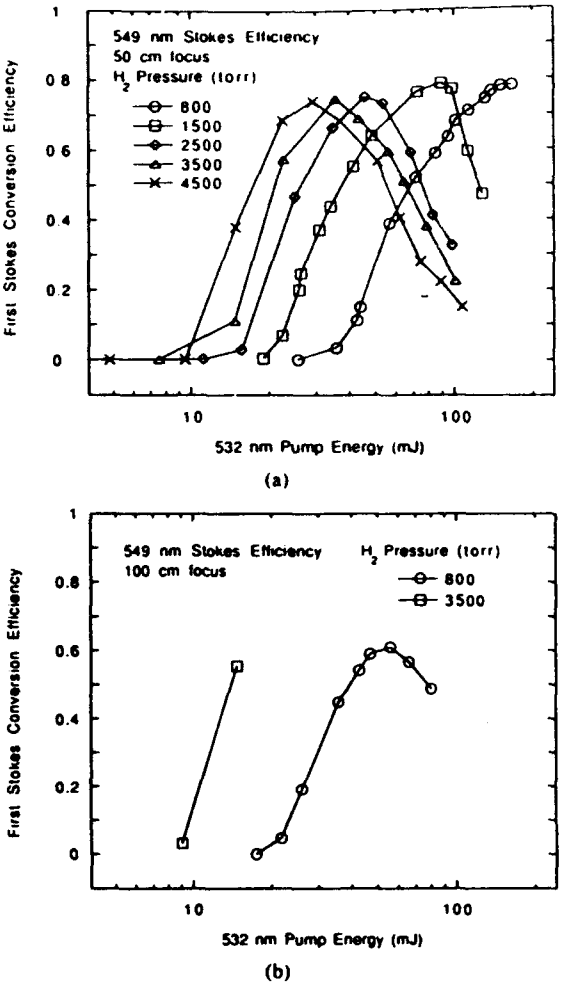


Fig. 3. Raman conversion efficiency in $H_2$ with (a) a 50-cm focusing lens, and (b) a 100-cm focusing lens.

narrower as higher order Raman processes reached threshold sooner. This effect was more pronounced with the longer 100 cm focusing lens. In this case, a threshold of ~10 mJ was obtained; however, the maximum conversion was only 60%.

The results for $D_2$ and HD are shown in Figs. 4 and 5, respectively. The gain for these gases was significantly less than for $H_2$ and a 100-cm focusing lens was used for most of the work. Here, the best conversion was achieved at the highest pressure. The $S_1(2)$ threshold in $D_2$ at 544 nm is ~20 mJ, compared to ~70 mJ for $S_1(1)$ in HD at 545 nm. This is consistent with the much larger linewidth for HD. Maximum conversion was 75% for $D_2$ and 64% for HD. It is interesting to note that even in HD the threshold decreases significantly from 1 to 3 amagats, although the pressure dependence is not as great as for $H_2$ and $D_2$.

For each of the hydrogen species, the pump threshold was found to decrease with increasing pressure as expected in this pressure range. We also observed significantly lower thresholds for the longer focal length lens in contrast to generally accepted ideas. If Stokes and anti-Stokes coupling is neglected, the single-pass gain is predicted to vary as $\tan^{-1}[L/b]$, where $L$ is the gain path

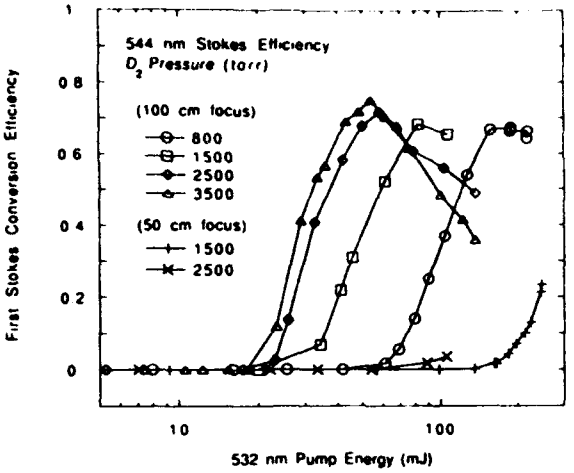


Fig. 4. Raman conversion efficiency in $D_2$.

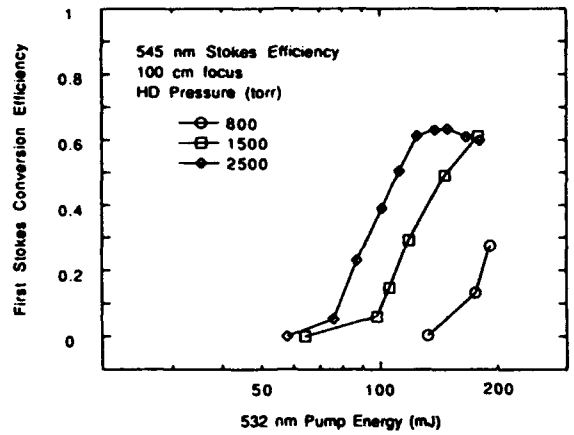


Fig. 5. Raman conversion efficiency in HD.

length and $b$ is the confocal parameter of the pump [14], [15]. However, in our experiments $b$ ranged from 1 cm to 4 cm and the cell length was 100 cm, which means that we were always operating in the short confocal length limit where $\tan^{-1}[L/b]$ is insensitive to $b$. One possible explanation for our observed threshold behavior might be greater Stokes and anti-Stokes coupling and gain suppression with the shorter focal length lens [16].

## IV. Conclusion

Stimulated rotational Raman conversion has been efficiently demonstrated in all three molecular hydrogen isotopes with a 532 nm Q-switched pump source. Optimum gas pressures and pump focusing have been determined. Single pass conversion efficiencies of 80%, 75%, and 64% have been achieved to the first Stokes wavelengths with $H_2$, $D_2$, and HD, respectively. The maximum efficiency is generally limited by further Raman conversion of the initially generated Stokes light. The thresholds were found to increase in the order $H_2 < D_2 < HD$ as expected. With the 100 cm lens, the threshold for HD is ~8 times that for $H_2$. This is about 50% less than would be predicted from the steady-state gains of Fig. 1 due to the more transient nature of the Raman gain for $H_2$. The relative thresholds of $H_2$ and $D_2$ are reasonably consistent with the calculated steady-state gains based on the population statistics and the linewidth data.

In conclusion, intermediate frequency shifts such as these may be useful by themselves, or in combination with other nonlinear techniques, as methods to achieve specific wavelengths for system applications. In a space environment, the Raman cells could also be operated at lower temperatures and additional frequency shifts would be practical.

## References

[1] J. A. Gelbwachs, "Atomic resonance filters," *IEEE J. Quantum Electron.*, vol. QE-22, pp. 1266-1277, 1988.

[2] E. L. Kerr, "Fraunhofer filters to reduce solar background for optical communications," *Opt. Eng.*, vol. 28, pp. 963-968, 1989.

[3] F. E. Hanson, D. L. Katz and P. Poirier, "Feasibility of a 486 nm Fraunhofer laser source based on a $^4F_{3/2} \rightarrow {}^4I_{9/2}$ neodymium laser," NRaD Tech. Rep. 1480, Mar. 1992.

[4] S. R. Bowman, B. J. Feldman, J. M. McMahon, A. P. Bowman, and D. Scarl, in *Tunable Solid State Lasers*, Vol. 5 of the OSA proceeding Series, M. L. Shand and H. P. Jensen, Eds. Washington, DC: Optical Society of America, 1989, p. 108.

[5] E. Gregor, O. Kahan, and D. W. Mordaunt, "Efficient rotational Raman conversion in hydrogen, deuterium, and hydrogen/deuterium mixes using a phase conjugate pump laser," in *Conference for Lasers and Electro-Optics, 1989 Technical Digest Series, Vol. 11.* Washington, DC: Optical Society of America, 1989, p. 384.

[6] G. Herzberg, *Molecular Spectra and Molecular Structure I. Spectra of Diatomic Molecules*. Princeton, NJ: D. Van Nostrand Company, 1950.

[7] B. P. Stoicheff, "High resolution Raman spectroscopy of gases, IX. Spectra of $H_2$, HD, and $D_2$," *Can. J. Phys.*, vol. 35, pp. 730-741, 1957.

[8] M. Rokni and A. Flusberg, "Stimulated rotational Raman scattering in the atmosphere," *IEEE J. Quantum Electron.*, vol. QE-22, pp. 1102-1108, 1986.

[9] G. C. Herring, M. J. Dyer, and W. K. Bischel, "Temperature and density dependence of the linewidths and line shifts of the rotational Raman lines in $N_2$ and $H_2$," *Phys. Rev. A*, vol. 34, pp. 1944-1951, 1986.

[10] W. K. Bischel and M. J. Dyer, "Temperature dependence of the Raman linewidth and line shift for the Q(1) and Q(0) transitions in normal and para-$H_2$," *Phys. Rev. A*, vol. 33, pp. 3113-3123, 1986.

[11] K. D. Van Den Hout, P. W. Hermans, E. Mazur, and H. F. P. Knaap, "The broadening and shift of the rotational Raman lines for hydrogen isotopes at low temperatures," *Physica*, vol. 104A, pp. 509-547, 1980.

[12] M. D. Duncan, R. Mahon, L. L. Tankersley, and J. Reintjes, "Transient stimulated Raman amplification in hydrogen," *J. Opt. Soc. Am B*, vol. 5, pp. 37-52, 1988.

[13] W. R. Trutna, Jr., Y. K. Park, and R. L. Byer, "The dependence of Raman gain on pump laser bandwidth," *IEEE J. Quantum Electron.*, vol. QE-15, pp. 648-655, 1979.

[14] D. Cotter, D. C. Hanna and R. Wyatt, "Infrared stimulated raman generation: Effects of gain focussing on threshold and tuning behaviour," *Appl. Phys.*, vol. 8, pp. 333-340, 1975.

[15] W. R. Trutna and R. L. Byer, "Multi-pass Raman Gain Cell," *Appl. Optics*, vol. 19, p. 301, 1980.

[16] B. N. Perry, P. Rabinowitz, and D. S. Bomse, "Stimulated Raman scattering with a tightly focussed pump beam," *Opt. Lett.*, vol. 10, pp. 146-148, 1985.

**Frank Hanson**, photograph and biography not available at the time of publication.

**Pete Poirier**, photograph and biography not available at the time of publication.